Science of the Total Environment 856 (2023) 158974

Contents lists available at ScienceDirect

Science of the Total Environment

journal homepage: www.elsevier.com/locate/scitotenv

Determinants of spatial variability of air pollutant concentrations in a street canyon network measured using a mobile laboratory and a drone

Leena Järvi [a,b,*], Mona Kurppa [c], Heino Kuuluvainen [d], Topi Rönkkö [d], Sasu Karttunen [a], Anna Balling [a], Hilkka Timonen [e], Jarkko V. Niemi [f], Liisa Pirjola [a,g]

[a] Institute for Atmospheric and Earth System Research/Physics, Faculty of Science, University of Helsinki, P.O. Box 64, Helsinki 00014, Finland
[b] Helsinki Institute of Sustainability Science, University of Helsinki, P.O. Box 4, Helsinki 00014, Finland
[c] Kjeller Vindteknikk, Tekniikantie 14, Espoo 02150, Finland
[d] Aerosol Physics Laboratory, Physics Unit, Faculty of Engineering and Natural Sciences, Tampere University, P.O. Box 692, Tampere 33014, Finland
[e] Atmospheric Composition Research, Finnish Meteorological Institute, P.O. Box 503, Helsinki 00101, Finland
[f] Helsinki Region Environmental Services Authority, Ilmalantori 1, Helsinki 00240, Finland
[g] Department of Automotive and Mechanical Engineering, Metropolia Applied University, P.O. Box 4071, Vantaa 01600, Finland

HIGHLIGHTS

- The spatial variability of air pollutant concentrations was experimentally evaluated using observations from a mobile laboratory and a drone
- We observed that both mean flow and turbulent fluctuations need to be considered when pollutant dispersion and concentrations are examined
- Thermal turbulence has strong impact particularly on the formation of aerosol particle hotspots in winter
- Prediction equations for vertical pollutant decay in a wide street canyon were developed
- The vertical decay was mostly controlled by seasonal variations in air temperature over mean flow and turbulent processes

GRAPHICAL ABSTRACT

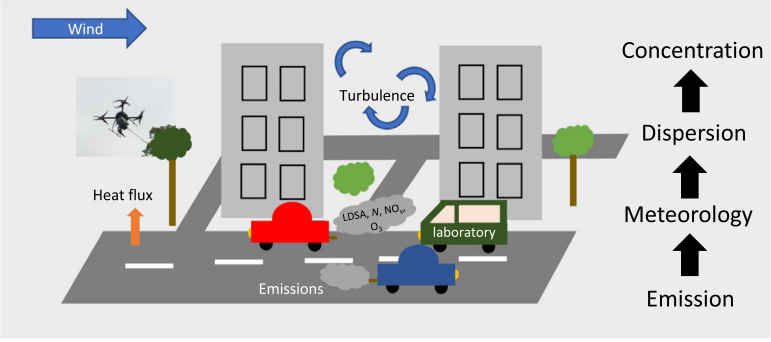

ARTICLE INFO

Editor: Jianmin Chen

Keywords:
Air quality
Drone
Meteorology
Mobile laboratory
Turbulence

ABSTRACT

Urban air pollutant concentrations are highly variable both in space and time. In order to understand these variabilities high-resolution measurements of air pollutants are needed. Here we present results of a mobile laboratory and a drone measurements made within a street-canyon network in Helsinki, Finland, in summer and winter 2017. The mobile laboratory measured the total number concentration (*N*) and lung-deposited surface area (LDSA) of aerosol particles, and the concentrations of black carbon, nitric oxide (NO_x) and ozone (O_3). The drone measured the vertical profile of LDSA. The main aims were to examine the spatial variability of air pollutants in a wide street canyon and its immediate surroundings, and find the controlling environmental variables for the observed variability's.

The highest concentrations with the most temporal variability were measured at the main street canyon when the mobile laboratory was moving with the traffic fleet for all air pollutants except O_3. The street canyon concentration levels were more affected by traffic rates whereas on surrounding areas, meteorological conditions dominated. Both the mean flow and turbulence were important, the latter particularly for smaller aerosol particles through LDSA and *N*. The formation of concentration hotspots in the street network were mostly controlled by mechanical processes but

* Corresponding author at: Institute for Atmospheric and Earth System Research/Physics, Faculty of Science, University of Helsinki, P.O. Box 64, Helsinki 00014, Finland.
E-mail address: leena.jarvi@helsinki.fi (L. Järvi).

http://dx.doi.org/10.1016/j.scitotenv.2022.158974
Received 22 April 2022; Received in revised form 16 September 2022; Accepted 19 September 2022
Available online 27 September 2022

in winter thermal processes became also important for aerosol particles. LDSA showed large variability in the profile shape, and surface and background concentrations. The expected exponential decay functions worked better in well-mixed conditions in summer compared to winter. We derived equation for the vertical decay which was mostly controlled by the air temperature. Mean wind dominated the profile shape over both thermal and mechanical turbulence. This study is among the first experimental studies to demonstrate the importance of high-resolution measurements in understanding urban pollutant variability in detail.

1. Introduction

Deteriorated air quality in urban areas is one of the major global challenges we are facing today. Adverse health effects including respiratory and cardiovascular diseases are coupled to several air pollutants with particulate matter being the most important. The sources of air pollutants in urban areas have largely been identified, but our ability to understand their spatial and temporal distributions within urban areas especially at local scale is limited. To ensure healthy and safe living environment in cities we need in-depth understanding on the factors controlling pollutant dispersion, and their high spatial and temporal variability, in addition to effective means to reduce pollutant emissions.

Road traffic is a dominant source for both gaseous and particulate air pollutants in urban areas (e.g. Kittelson et al., 2004; Fenger, 2009). As a consequence, highest pollution levels are commonly seen at the pedestrian level in street canyons due to proximity of the emissions (Vardoulakis et al., 2003). This especially when the prevailing meteorological conditions and turbulent mixing lead to inefficient pollutant transport from the street canyon and mixing of the above air towards the surface (Britter and Hanna, 2003). The turbulent properties and scalar transport of the flow are furthermore modified by morphological effects such as building layouts and vegetation (Barlow et al., 2004; Kurppa et al., 2018; Karttunen et al., 2020), creating spatially and temporally variable concentration fields (Vardoulakis et al., 2005; Pirjola et al., 2012; Borge et al., 2016). The main features of pollutant dispersion have been studied (Li et al., 2021), but we still have gaps in fundamental understanding of the processes controlling the mixing conditions and pollutant distributions. This particularly in realistic urban areas as most of past studies have been made in wind tunnels or they have focused on idealised building arrays using computational fluid dynamics (CFD). These studies have shown how local dispersion is a result of mechanical and thermal effects but experimental evidence of their dominance in different meteorological conditions in real urban conditions has been missing. Recently, Barbano et al. (2021) conducted a field campaign in Bologna, Italy, where they found thermal processes to take place faster than the mechanical ones, and that thermal effects are particularly efficient for perpendicular wind directions.

Furthermore, we are often lacking information on the effect of dispersion on different aerosol metrics representative for different sized of aerosol particles. The local concentrations of smaller particles are most complicated as their local distributions are shaped by the different transformation processes such as nucleation, coagulation, condensation and deposition (Kumar et al., 2011). It has been found that indeed the dispersion is somewhat different for smaller and larger particles (Rivas et al., 2017; Karttunen et al., 2020) indicating the need to examine in detail what factors control different aerosol metrics.

One reason for the lack of experimental evidence is that typically air quality measurements in urban areas are conducted in a few air quality stations within a city, whereas in order to examine pollutant distributions in detail observations with high spatial and temporal resolution are needed. Information on the spatial variability at local scale has been obtained in the past by conducting stationary measurement campaigns (Vardoulakis et al., 2005; Borge et al., 2016), or using novel measurement platforms such as mobile laboratories (e.g. Pirjola et al., 2012; Ruths et al., 2014; Choi et al., 2016; Solomon et al., 2020) or drones (Liu et al., 2021; Kuuluvainen et al., 2018) which allow higher spatial resolution than stationary measurements but are limited to shorter measurement periods.

To answer the needs above, this study examined the horizontal and vertical variability of air quality components measured using a mobile laboratory and a drone in a wide boulevard-type street canyon in Helsinki and its adjacent road network under contrasting meteorological conditions. Particularly, we wanted to distinguish the most important factors impacting the dispersion of different pollutants including aerosol particle number, black carbon (BC) and lung-deposited surface area (LDSA) of aerosol particles. Particle number, LDSA concentrations and BC concentrations are typically dominated by relatively small particle sizes, being efficiently deposited to human respiratory system, and thus tried to be linked to the health effects of particles. Particulate mass (PM) is the only regulated aerosol variable and thus the most commonly measured and used in epidemiological studies, whereas there are indications that the metrics representing the smaller particle sizes could be more important factor when considering the harmfulness of PM (Oberdorster et al., 2005; Kuula et al., 2020).

2. Methods and material

Two intensive measurement campaigns to map the spatial variability of air pollutants were carried out in a busy street canyon and its immediate surroundings in Helsinki, Finland, in 2017 (Fig. 1). The measurements were conducted next to an urban air quality monitoring supersite (60°110N, 24°570E) located in a street canyon and operated by the Helsinki Region Environmental Services Authority (HSY). The street canyon has pavement and three lanes for both directions. The outermost lane next to the pavement is reserved for buses and taxis. In the middle of the street canyon, there are two tram lines surrounded by street trees. The width of the street canyon is 42 m, and building heights next to the HSY supersite are 19 m and on the other side of the canyon 16 m. The average height-to-width ratio of the canyon is 0.45.

The first campaign took place from 5 till 16 June 2017 and the second from 27 November till 8 December 2017. During the measurement campaigns, a mobile laboratory Sniffer (Pirjola et al., 2004) and a drone were used to map the horizontal and vertical variability of gaseous compounds (only mobile laboratory) and aerosol particles. Stationary measurements included air quality and turbulence observations made at the HSY supersite and background station SMEAR III Kumpula (Järvi et al., 2009) located 900 m north from the main monitoring site (Fig. 1). All mobile laboratory and drone measurements were made on non-rainy workdays.

2.1. Mobile laboratory

A mobile laboratory "Sniffer" (VW LT35 diesel van) (Pirjola et al., 2004, 2012) measured the horizontal variability of air pollutants with 1 s resolution on 14 workdays during the measurement campaigns. On each day, Sniffer collected data for 2 h up to three times a day (during morning and afternoon rush hours and early evening) allowing different meteorological conditions to be covered. During each 2-hour period, Sniffer circulated an area of a few blocks around the HSY supersite (Fig. 1). Furthermore, the mobile laboratory stopped one to two times with engine off to measure the background concentrations away from the road emissions and on both sides of the main street canyon for >5 min.

The inlets of the instruments were positioned above the van's windshield, 2.4 m above the ground. The aerosol particle number size distribution used to calculate the lung deposited surface area (LDSA) was measured using an electrical low-pressure impactor (ELPI, Dekati Ltd., Finland) equipped with a filter stage (Lappi et al., 2002) and an additional stage

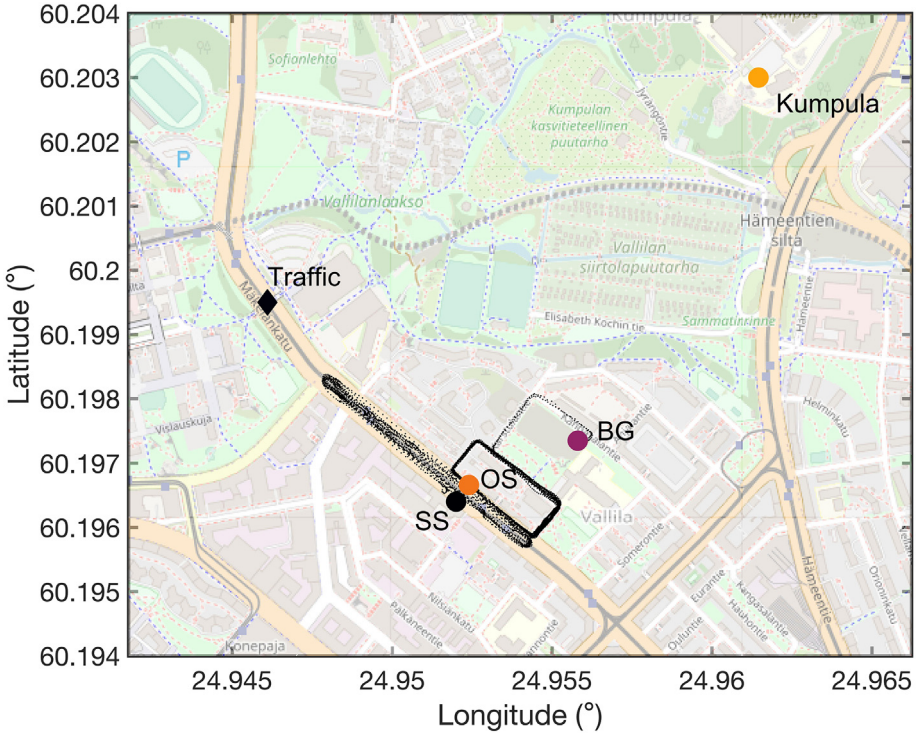

Fig. 1. Map of the measurement area. Mobile laboratory driving route on 14 June 2017 afternoon is plotted for visualisation. SS and OS mark the drone locations at the HSY supersite and opposite it. BG is the background location for the mobile laboratory where standing background measurements were collected. In Kumpula SMEAR III the stationary air quality and turbulence measurements were collected and Traffic marks the location for traffic rate measurements. @OpenStreetMap contributors.

designed to enhance nanoparticle size resolution (Yli-Ojanperä et al., 2010). LDSA concentrations strongly correlate with ion attachment and diffusion charging, and thus can be measured with diffusion charger based instruments such as ELPI. LDSA is calculated by summing up the electric currents measured with ELPI by multiplying used currents with field calibration coefficient 60 $\mu m^2/(cm^3$ pA) (Kuuluvainen et al., 2016). ELPI measured the currents at aerodynamic size range 7 nm–10 μm but only currents from 7–950 nm were used to calculate the LDSA. The total number concentration (N) with particles larger than 2.5 nm was measured with a condensation particle counter CPC (TSI3776, TSI Ltd., USA), as well as the concentrations of nitrogen oxides (NO, NO_2 and NO_x) using a chemiluminescence analyser (APNA360, Horiba Ltd., Japan) and ozone (O_3) using a UV absorption analyser (O3 42 M, Environment, France). Black carbon (BC) in PM1 size fraction was measured using an aethalometer (AE33, Magee Scientific, USA). Measurements at 880 nm were used for the BC concentrations. The van carried also a GPS to save the speed and driving route.

2.2. Drone measurements

Vertical distribution of LDSA was measured using a multicopter model X8 (VideoDrone Finland). The copter was modified for the purpose of emission measurements by replacing the main payload of the drone with a sensor unit containing an onboard computer, network modem, GPS antenna, and humidity, temperature, and pressure sensors. The pressure sensor was used as an altimeter with its accuracy ±0.12 hPa corresponding approximately ±1 m in altitude. In addition, particle sensor Partector (Naneos GmbH, Switzerland, Fierz et al., 2014) was installed to the drone measuring the aerodynamic size range 10–300 nm. Partector is based on the diffusion charging of particles and the induced current is measured with an electrometer. The output current signal is calibrated to measure the alveolar lung deposited surface area (LDSA) concentration. The weight of the Partector is 400 g, time resolution 1 s, and it can be operated as much as 15 h without recharging the battery. Air sample to the Partector was drawn through a 70 cm long inlet tube outside of air flow caused by rotors. Details of the measurement setup can be found from Kuuluvainen et al. (2018).

Drone measurements were made on four days during the measurement campaigns. The drone was always flown on both sides of the street canyon (Fig. 1) from the ground level to an altitude of 50 m with an approximate vertical velocity of 1 m/s. During a 2-hour measurement period, the drone was flown 10 subsequent up-and-down flights on each side lasting around 30 min after which the battery was changed or recharged. Two to four measurement periods were conducted on each day. The number of the 2-hour periods was affected by meteorological conditions or other challenges in the measurements.

To ensure the quality of the drone LDSA measurements, three similar Partectors were used as reference measurements. One Partector was located at the ground level next to the measurement container at the HSY supersite, one to the other side of the canyon next to the drone measurements, and one at the roof level of the other side. The same 1 s resolution was used in these measurements.

2.3. Stationary measurements

Stationary air quality measurements were conducted at the HSY supersite located in the main street canyon. The station has a measurement container located on a pavement next to the road. Sample air for the measurement devices is taken from the roof of the container at a height of 4 m from the ground level. The aerosol particle number size distribution at size range 8–800 nm was measured using a differential mobility particle sizer (DMPS, Aalto et al., 2001) with a 9 min temporal resolution. In DMPS, aerosol particles are bipolarly charged, classified into different size classes based on their electrical mobility and finally counted using a CPC. LDSA was measured using a Pegasor AQ Urban sensor (Pegasor, Finland), representing aerosol sizes 10–400 nm, BC using a Multi Angle Absorption Photometer (MAAP 5012, Thermo Scientific, USA), the concentrations of NO, NO_2 and NO_x using a chemiluminescence analyser (APNA 370), and O_3 using a UV absorption analyser (APOA 370, Horiba) with 1-min temporal resolution. For the duration of the measurement campaigns, a 3-dimensional ultrasonic anemometer (USA-1, Metek GmbH, Germany) to provide wind components (u, v, w) and sonic temperature at high temporal

resolution (10 Hz) was installed on northern corner of the container on top of a pole resulting total height of the turbulence measurements at 5 m.

Additional stationary measurements representative for urban background were collected at the SMEAR III Kumpula station (Järvi et al., 2009). At this site, the aerosol particle number size distribution at size range 3–1000 nm was measured using a twin DMPS and BC using the same aethalometer model as at the mobile laboratory. The concentration of NO_x was measured using a chemiluminescence analyser (TEI42S, Thermo Instruments, USA). The instruments were located in a measurement container and the sample air was drawn from the instruments above the container at height of 4 m. DMPS and aethalometer measured with 10-min temporal resolution, and NO_x instrument with 1 min temporal resolution. Turbulence variables were measured using a similar ultrasonic anemometer as at the HSY supersite on top of a 31 m high measurement tower (Järvi et al., 2009; Nordbo et al., 2012).

Traffic count was measured in 15-min time resolution by the City of Helsinki at the main street canyon 600 m north of the HSY supersite (Fig. 1).

2.4. Data analysis

2.4.1. Turbulence data

The high-frequency wind and temperature measurements at the background station and the HSY supersite were used to calculate turbulence parameters describing dispersion conditions. The used parameters included mean wind speed (U, m s^{-1}), vertical wind speed variance (σ_w, m s^{-1}), momentum flux ($\overline{u'w'}$, m^2 s^{-2}), sensible heat flux (Q_H, W m^{-2}) and atmospheric stability (ζ). The last two were calculated from covariances between the vertical wind speed (w) and the respective scalar of interest following

$$Q_H = \rho_w c_p \overline{(T_s' w')}, \tag{1}$$

$$\zeta = -\frac{z\kappa g \overline{(T_s' w')}}{T_s u_*^3}, \tag{2}$$

where the overbar indicates time average which in our case is either 10 or 30 min, $'$ indicates the fluctuation of a scalar from its mean, u and v are the Eastern and Northern wind components (m s^{-1}), ρ_w is the air density (kg m^{-3}), $c_p = 1004\,\mathrm{J\,kg^{-1}K^{-1}}$ is the specific heat of air at constant pressure, T_s the sonic temperature (K), z is the measurement height (m), κ Von Karman constant (0.41), g is the gravity (9.81 m s^{-2}) and u_* is the friction velocity defined as

$$u_*^2 = \sqrt{\overline{(u'w')}^2 + \overline{(v'w')}^2}. \tag{3}$$

In the calculations commonly accepted procedures including 2D coordinate rotation, despiking, cross-wind and heating (only in Kumpula where water vapour data were available) corrections and stationary filtering (60 % limit) were used (Nordbo et al., 2012). Atmospheric stability was used to estimate stability classes very unstable ($\zeta \le -2$), unstable ($-2 < \zeta \le -0.01$), neutral ($-0.01 < \zeta \le 0.01$), stable ($0.01 < \zeta \le 2$) and very stable ($\zeta > 2$).

2.4.2. Mobile laboratory

The raw data measured by the mobile laboratory were divided by driving routes. These were standing background (BG), main street canyon (MS), side streets (SD), main street canyon and side streets (MS + SD), standing the HSY supersite (SS) and standing opposite the HSY supersite (OS). The mobile laboratory stayed from 5 to 15 min at each driving route. Furthermore, the first 3 min of the standing measurements were always removed from the data analysis. Median values for each driving route at each time instance were calculated resulting in 701 data points all together. These median data were linearly fitted against 10 min meteorological and traffic data.

In addition to simple linear correlations of pollutant concentrations and environmental variables at different driving routes, a generalised linear multivariable regression was made. A linear model was chosen over other regression models for its transparency. Also linear regression model belongs to white-box models which have been reported to be closer to physics-based models and with them it is easier to spot the relative importance of the predictor variables (Fung et al., 2021). Furthermore, normalisation of the predicted variables (concentrations of LDSA, N, BC, NO_x and O_3) and the predictor (environmental) variables $X_1 \ldots X_2$ gives regression coefficients β_n telling the relative contribution of each environmental variable to the value of the predicted variable ($\widehat{P}$). The used linear regression model had form

$$\widehat{P} = \beta_0 + \beta_1 X_1 + \beta_2 X_2 + \ldots + \beta_n X_n. \tag{4}$$

We used bootstrapping to get error estimates for the model parameters and performance indices (Järvi et al., 2008). In bootstrapping, the data were divided into 100 subsets each including arbitrary 5/6 of the original data. Separate regression model for each subset was constructed and the final statistics calculated as medians, and 25th and 75th percentiles of each subset. To find appropriate variables to the regression model, a sequential forward feature selection was used (e.g. Lange et al., 2021). The feature selection selects a subset of variables from the initial variable set that best predict the data by sequentially selecting features which improve the prediction. We tested both forward selection and LASSO to select suitable variables for the regression, but the first was chosen over the latter as LASSO has been reported to trade off potential bias in estimating individual parameters for better overall prediction. Thus, there might be issues in reliable estimation of the regression coefficients and interpretation of the contribution of individual variables (Ranstam and Cook, 2018). The variables included to the initial set were background meteorological (air temperature T_{air}, mean wind speed U and wind direction) and turbulent (Q_H and $\overline{u'w'}$) variables, and the traffic rate. Wind direction was divided into eight classes (so called dummy variable) relative to the street canyon ($330-20^\circ, 20-60^\circ, 60-110^\circ, 110-150^\circ, 150-200^\circ, 200-240^\circ, 240-290^\circ, 290-330^\circ$). Here $\overline{u'w'}$ was chosen to describe turbulent fluctuations over σ_w as it describes also the mechanical turbulence production. Correlation between $\overline{u'w'}$ and σ_w was strong with $R^2 = 0.72$. Street-canyon measurements were not included in the initial set of variables as they had strong linear correlations with the respective background variables and they present the local conditions at SS. Forward selection and linear regression were separately made for the two seasons.

In addition to temporal averaging of the raw data by driving route, data were spatially averaged to 4-m grids in order to examine the spatial variability of pollutant concentrations and formation of pollutant hotspots in detail. This was done based on the GPS information of the van. This resulted in all together 159 spatial maps. Meteorological data were averaged for each measurement period presenting the meteorological conditions for the 159 spatial maps. Forward selection of the most important environmental variables for each four meter grid was conducted using the same initial variable dataset as above. Grids for which forward selection was made needed to have in minimum 40 measurement points. For these grids the same linear regression model was fitted to obtain the relative contribution of meteorological variables and traffic rate to the different pollutant concentrations in each four-meter grid.

2.4.3. Vertical profiles

In order to examine the vertical dispersion of particles in the main street canyon, geometric mean values of LDSA vertical profiles over the 10 repetitions on each side of the canyon were calculated. This resulted in all together 37 profiles: 20 profiles from summer and 17 from winter. These were fitted against the height using a first-order exponential decay equation (Murena and Vorraro, 2003; Kumar et al., 2008; Kuuluvainen et al., 2018)

$$(C_z - C_f)/(C_0 - C_f) = exp(-zk/H), \tag{5}$$

where C_z is the LDSA at height z, C_0 is the LDSA at the ground level, C_f is the background LDSA, H is the canyon height and $k_1 = k/H$ is the exponential decay coefficient (m^{-1}) combining the meteorological and morphological effects of pollutant dispersion. The inverse of the decay function is the characteristic dispersion height. To find the value of k for each measured profile, a non-linear least-square regression to Eq. (5) was made.

Furthermore, a generalised linear regression model to predict k using meteorological variables was developed in similar fashion for the data measured by the mobile laboratory. A sequential forward feature selection was made using the same initial set of variables as before with the addition of having side of the street canyon (1 = SS, 2 = OS) and season (1 = summer, 2 = winter) as predicting variables. Here data from summer and winter were combined due to the small amount of data. In our case the morphology of the measurement sites on both sides of the main street canyon remains the same allowing to examine the effect of meteorology on pollutant vertical dispersion in detail.

3. Results and discussion

Besides general data analysis of the measurement campaigns, we chose two measurement periods (hereafter called case examples) to visualize the behaviour of analysed variables. One case example from each season was selected representing the typical behaviour of air pollutant concentrations with moderate wind speeds. The two case examples were afternoons on 14th June and 5th December.

3.1. Meteorological conditions

During the summer campaign, the background air temperature (T_{air}) was on average 14.7°C and reached 22.3°C, whereas in winter T_{air} remained below 5.4°C with a mean value of 1.7°C (Fig. 2 a–b). During both campaigns slightly warmer temperatures were measured in the street canyon (on average 14.9 and 2.3°C, respectively) due to anthropogenic heat emissions from traffic and buildings, and solar radiation wrapping due to reduced sky-view factor. During the summer campaign, mean wind (U) was slightly calmer than during the winter campaign with the background averages being 3.3 and 5.1 m s^{-1}, respectively (Fig. 2 c–d). In the street canyon, U were lower being on average 0.8 and 1.6 m s^{-1}. Prevailing wind direction was from west–north-west and east–south-east during the campaigns, respectively (Fig. 1 in the Supplementary material). Eastern and western flows are perpendicular to the street canyon allowing formation of canyon vortex whereas south-east and north-west are parallel to the street canyon.

As measurements were only made on dry days, there were often clear sky conditions (Fig. 2 e–f). The large contrast between the summer and winter campaign radiation levels had strong effect on the atmospheric stability and appearance of different stability classes (Fig. 3). During summer campaign, very stable atmosphere indicating limited vertical mixing was mostly seen at nighttime whereas in daytime very unstable conditions occurred 93 % on midday (between 11:00–14:00) indicating well-mixed lower atmosphere. In winter the atmosphere remained less unstable in daytime with very unstable conditions occurring 20 % and unstable conditions occurring

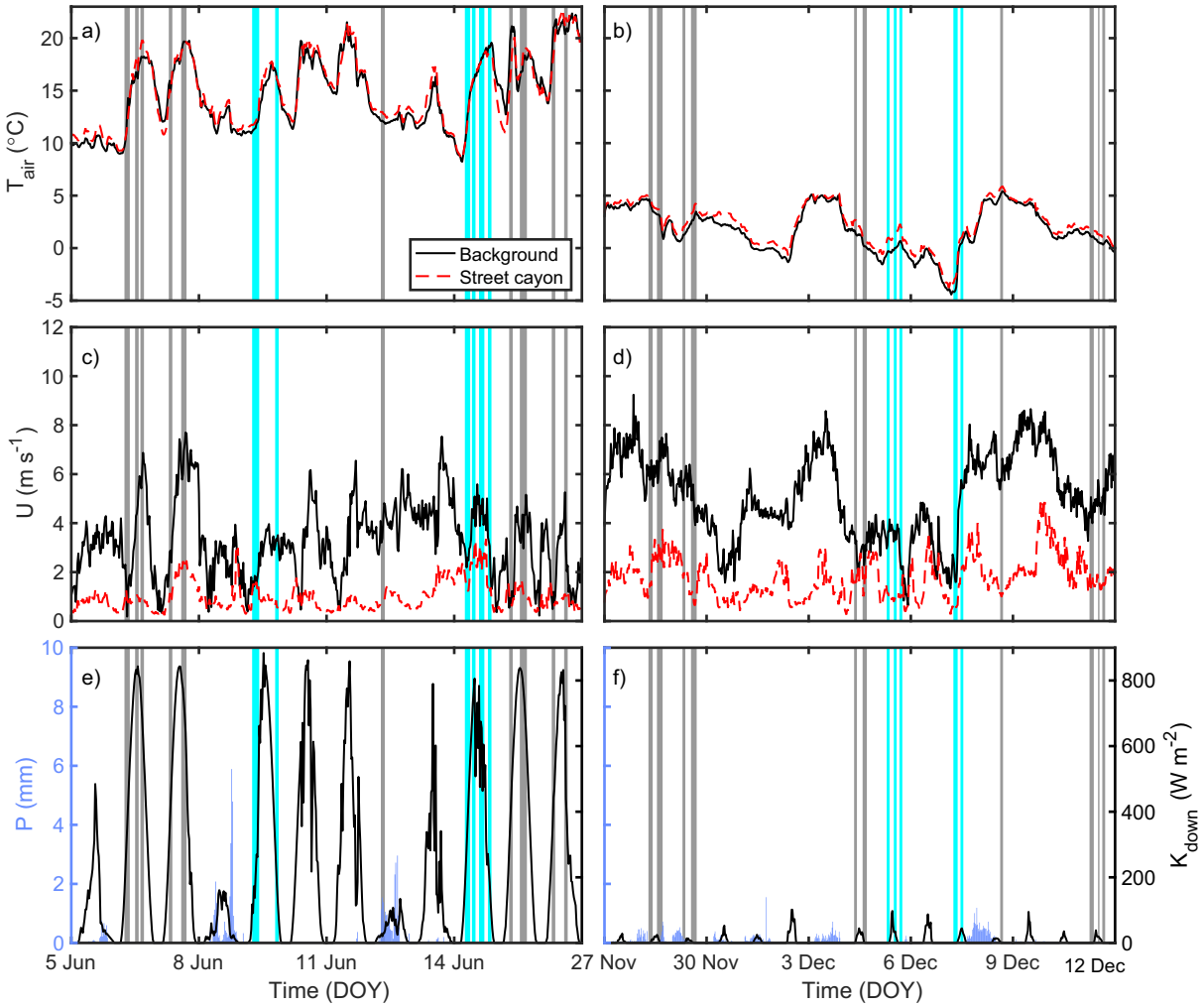

Fig. 2. Time series of 30-min air temperature (T_{air}, °C) (a–b) and mean wind speed (U, m s^{-1}) (c–d) measured at the background SMEARIII Kumpula station and the HSY supersite, and precipitation (P, mm) and solar radiation (K_{down}, W m^{-2}) (e–f) measured at the background station during the summer (a, c, e) and winter (b, d, f) measurement campaigns. Grey areas show the times for mobile laboratory measurements and turqoise areas the times for mobile laboratory + drone measurements.

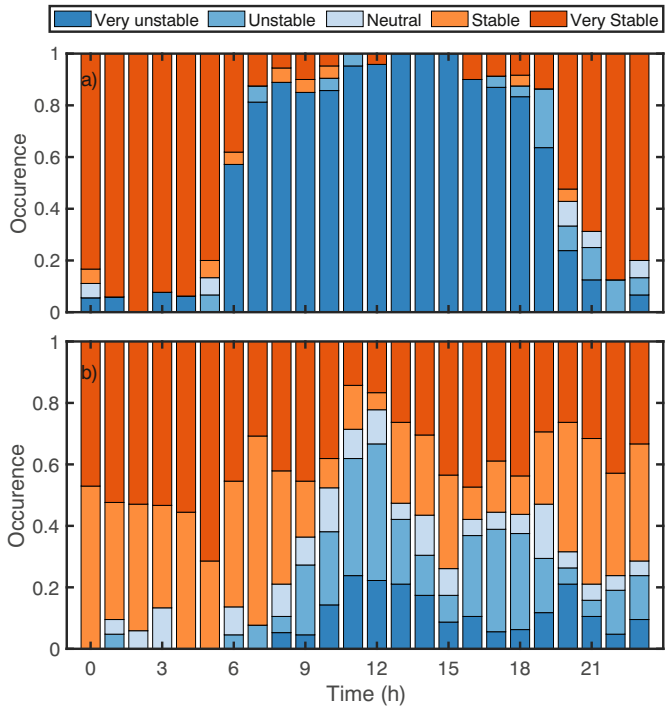

Fig. 3. Diurnal occurrence of different atmospheric stability classes (very unstable: $\zeta \leq -2$, unstable: $-2 < \zeta \leq -0.01$, neutral: $-0.01 < \zeta \leq 0.01$, stable: $0.01 < \zeta \leq 2$ very stable:$\zeta > 2$) at the background SMEARIII Kumpula station during the summer (a) and winter (b) measurement campaigns.

35 % on midday. Also the onset of mixing was later in winter (around 9:00) than in summer (around 6:00). Thus, in summer the mixing conditions are very different compared to winter which will have direct impact on vertical dispersion and studied pollutant concentrations.

The contrast in meteorological conditions between the winter and summer campaigns was also visible in our case examples (Fig. 2 in the Supplementary material). The mean daily T_{air} during the summer case example was 14.7°C and during winter case example −0.5°C. The street canyon T_{air} was similar to background T_{air} in summer (14.9°C) but clearly larger in winter (1.3°C). The greater thermal turbulence generation in summer was seen in Q_H which reached 270 and 180 W m^{-2} at the background and street-canyon compared to −5 and 6 W m^{-2}, respectively, in winter. U was similar between the two case examples (3.5 and 2.0 m s^{-1} at the background, 1.8 and 1.1 m s^{-1} in the street-canyon) but stronger turbulence was seen in summer when compared to winter. Thus, there were more both mechanical and thermal mixing in summer than in winter creating more favorable conditions for pollutant dispersion. Wind was from the North (mean 356°) and thus around 45° relative to the main street canyon in summer, and from the West (mean 282°) in winter being slightly more parallel to the street canyon than in summer. At the time of the mobile laboratory and drone measurements, U decreased and turned more from south-west during the winter case example.

3.2. Horizontal variability of pollutant concentrations

The air pollutant concentrations measured by the mobile laboratory showed large temporal and spatial variability (Table 1, Fig. 6 in the Supplementary material). Excluding O_3 and N in summer ($30 \cdot 10^3$ cm^{-3} at OS), the highest concentrations were measured at the main street canyon, when the van was moving with the traffic, with median LDSA 73 and 66 μm^2 cm^{-3}, N 27 and $29 \cdot 10^3$ cm^{-3}, BC 2.2 and 2.2 μg m^{-3}, and NO_x 55 and 72 ppb in summer and winter, respectively. The lowest concentrations were systematically measured at BG when the mean values were also closest to the concentrations measured at the background SMEARIII Kumpula station. The median concentrations remained below 37 μm^2 cm^{-3} (LDSA), $11 \cdot 10^3$ cm^{-3} (N), 0.7 μg m^{-3} (BC) and 13 ppb (NO_x). On other driving routes the concentrations remained between these limits with highest concentrations commonly measured at OS in summer and on the combination route MS + SD in winter. In the case of O_3, lowest concentrations were measured at the main street canyon (17 ppb in summer and 8.2 ppb winter) and largest at the BG (27 ppb in summer and 13 ppb winter) due to photochemical reactions with nitrogen compounds. For the same reason, O_3 concentrations were greater in summer than in winter. For N, BC and NO_x higher concentrations were measured in winter than in summer whereas for LDSA in summer (excluding OS). As the traffic rates are similar between the two campaigns (15-min mean vehicle count 675 in winter and 658 in summer) the larger wintertime concentrations can be explained by variability in emission factors in different temperatures and the limited mixing in winter. Traffic flow towards the city centre passes the HSY supersite in the morning and opposite the HSY supersite in the afternoon. Earlier study from Helsinki also found greater LDSA in summer than in winter due to larger particle sizes (Kuula et al., 2020) as relevant particle sizes likely due to increased photochemistry and VOC emissions (Barreira et al., 2021). All the measured concentrations were typical for near-road environments (e.g. Pirjola et al., 2012; Eeftens et al., 2015; Borge et al., 2016; Rivas et al., 2020) with the highest concentrations at major roads and decay in concentrations the further from the emission sources you go (Ruths et al., 2014; Enroth et al., 2016; Amato et al., 2019). While standing at SS, LDSA measured by ELPI correlated well (r = 0.64, RMSE = 29.6 μm^2 cm^{-3}) with the stationary Pegasor instrument located at the HSY supersite but showed slightly larger concentrations (Mean bias error (MBE) = 3.3 μm^2 cm^{-3}) (Supplementary material Fig. 1). The observed differences between the two instruments were reasonable as they have different measurement principles, measurement heights and representative size ranges.

Table 1
Median concentrations of lung deposited surface area (LDSA), total particle number concentration (N), black carbon (BC), nitrogen oxides (NO_x) and ozone (O_3) on different driving routes during the summer and winter measurement campaigns. BG = standing background, MS = main street canyon, SD = side streets, MS + SD = main street canyon + side streets, SS = standing the HSY supersite, OS = standing opposite the HSY supersite.

		LDSA (μm^2 cm^{-3})	N (10^3 cm^{-3})	BC (μg m^{-3})	NO_x (ppb)	O_3 (ppb)
Summer	BG	36.5 ± 12.4	9.2 ± 3.5	0.6 ± 0.3	8.2 ± 5.0	27.4 ± 6.9
	MS	73.3 ± 23.1	27.4 ± 7.6	2.2 ± 1.0	54.8 ± 20.5	19.1 ± 7.7
	SD	43.8 ± 14.4	13.9 ± 6.9	1.2 ± 0.4	19.2 ± 9.5	20.4 ± 7.7
	MS + SD	61.7 ± 26.7	19.6 ± 4.6	1.5 ± 0.7	37.5 ± 20.4	21.9 ± 7.5
	SS	50.7 ± 15.7	17.6 ± 9.1	1.1 ± 0.3	27.6 ± 12.7	23.4 ± 4.7
	OS	63.1 ± 26.3	30.2 ± 14.3	1.8 ± 1.1	40.7 ± 25.2	16.6 ± 7.8
Winter	BG	25.4 ± 9.1	10.7 ± 3.4	0.7 ± 0.2	12.8 ± 4.9	13.0 ± 3.4
	MS	65.6 ± 20.7	29.2 ± 8.9	2.2 ± 0.7	71.8 ± 26.6	8.2 ± 3.8
	SD	34.3 ± 12.1	13.6 ± 4.3	1.1 ± 0.4	25.0 ± 12.9	11.4 ± 4.7
	MS + SD	51.2 ± 21.4	24.7 ± 7.2	1.8 ± 0.4	50.9 ± 18.7	10.2 ± 4.4
	SS	44.1 ± 17.7	27.4 ± 11.5	1.6 ± 0.6	47.2 ± 19.2	8.9 ± 4.7
	OS	43.4 ± 18.4	20.0 ± 8.2	1.3 ± 0.4	34.3 ± 24.7	11.9 ± 2.9

3.3. Controls of horizontal variability of pollutants

Pollutant concentrations at all driving routes showed varying correlations from meteorological variables (see Supplementary material). On both seasons, the linear correlations between different air pollutants and environmental variables were larger than that of traffic rates with greatest concentrations seen in cold and calm conditions. Depending on the air pollutant, largest linear correlation coefficients with traffic rate were seen in winter at SD (N, 0.19), SS (LDSA, 0.32) and MS (BC, 0.29; NO_x, 0.27). On other driving routes insignificant or even negative correlations were seen. In order to understand more in detail the effect of different variables at each driving route, linear regression between the different pollutant concentrations and environmental variables was made. Fig. 4 gives the beta coefficients of the variables affecting the pollutant concentrations identified by the forward selection on different driving routes. One should keep in mind that on some driving routes there was a small number of data points available which affects the certainty of the fit (Table 7 in the Supplementary material). Large variability in the most important variables for the measured pollutant, driving route and season was seen.

At BG, local road traffic had minor importance on the measured concentrations during both seasons and it was turbulent transport ($\overline{u'w'}$) which had most impact on pollutant levels excluding O_3. The BG concentrations increased with decreasing $\overline{u'w'}$ as the sign of $\overline{u'w'}$ is always negative with greater negative value indicating more turbulent mixing. For LDSA and *N*,

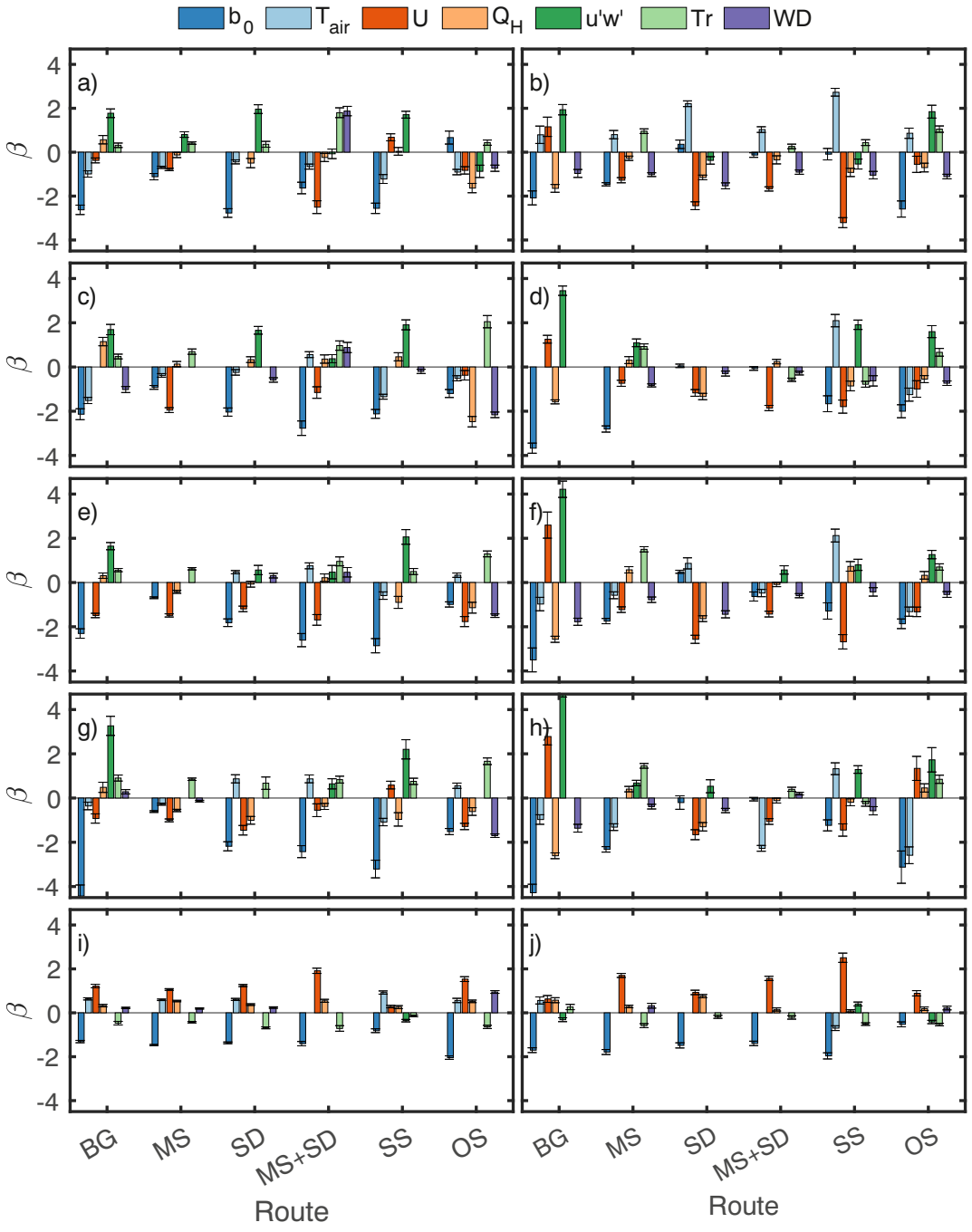

Fig. 4. Beta coefficients obtained from the multivariable linear fitting made between environmental variables air temperature (T_{air}), mean wind speed (U), sensible heat flux (Q_H), momentum flux ($\overline{u'w'}$), traffic rate (Tr) and wind direction (WD), and lung deposited surface area (a–b), total particle number (c–d), black carbon (e–f), NO_x (g–h) and O_3 (i–j) during summer (a, c, e, g, i) and winter (b, d, f, h, j). See Table 3 in the Supplementary material for detailed statistics.

T_{air} was the second important variable in summer and Q_H in winter. For BC and NO_x, U was the second important variable on both seasons. U and T_{air} were most important variables for O_3. At SD, $\overline{u'w'}$ dominated the concentrations of LDSA and N, and U the concentrations of BC, NO_x and O_3 in summer indicating the importance of pollutant transport from the main road either by turbulence or mean flow. In winter, U was important for all pollutant concentrations. It was the most important variable for all other concentrations than N which was slightly more affected by Q_H. Q_H was also important for BC and NO_x whereas T_{air} was more important for LDSA. At SD, wind direction was contributing largely to LDSA, BC and NO_x levels in winter emphasising the importance of pollutant transport from the main road in certain flow conditions. Traffic rate was important only for O_3. U was again the most important variable for O_3.

When driving with the traffic fleet at MS, traffic rate had greater contribution than on other driving routes. U was the most important variable in summer for other pollutants than LDSA which was slightly more affected by $\overline{u'w'}$. The mean wind was followed by traffic rate in the case of N, BC and NO_x. Traffic had the largest contribution to BC and NO_x in winter whereas for other pollutants either U (LDSA and O_3) or $\overline{u'w'}$ (N) contributed most. If the mobile laboratory was standing at the HSY supersite (SS) or opposite it (OS), the effect of road traffic decreased and the importance of meteorological variables increased. At SS, $\overline{u'w'}$ had the largest contribution to pollutant concentrations in summer except to O_3 which was most affected by T_{air}. T_{air} was also important for LDSA, N and NO_x. Thus, mean wind had little effect on the pollutant concentrations at SS in summer but rather concentrations were determined by mechanical turbulence and thermal effects. In winter, mean wind was more important than in summer being the most contributing variable for all other pollutants except for N which was most affected by T_{air}. T_{air} was second important variable for all other pollutants. At OS, the importance of Q_H increased in summer and it was the most important variable for LDSA and N. BC and O_3 on the hand were most affected by U, and NO_x by wind direction. Wind direction was also important for other pollutants. In winter, the importance of mechanical turbulence increased $\overline{u'w'}$ being the most important variable for LDSA, N and BC. NO_x was most affected by T_{air}. Other important variables varied between the different pollutants being wind direction for LDSA, T_{air} for N and BC, $\overline{u'w'}$ for NO_x and traffic for O_3. The differences in the explanatory variables at SS and OS could be explained by the different morphologies relative to the prevailing wind direction which is South-West. In this case, a street canyon vortex is formed causing pollutants to be pushed from OS to SS (Kurppa et al., 2020). Previous study found nanocluster concentrations to depend on wind direction at SS, but in their study they did not examine the relative importance of other meteorological variables (Hietikko et al., 2018). The SS side also gains more direct sun light in the morning while OS still remains in shadow, and in the afternoon the situation is vise versa with more radiation at OS than at SS.

The results show how the concentration levels at the main street canyon are more affected by traffic rates whereas on other driving routes environmental conditions dominate. Traffic rates were particularly important for NO_x. The result might be different if temporal correlations at a higher spatial resolution would have been examined whereas here we examined the effect of environmental variables on pollutant concentration medians at different routes. It is also evident that both mean flow and turbulent fluctuations contributed to the pollutant concentrations in the different driving routes emphasising the importance of turbulence in pollutant transport. For the aerosol metrics representing smaller particles, it was more often the mechanical turbulence which dominated over mean flow. O_3 concentrations were most often affected purely by mean wind. Traditionally, mainly due to lack of turbulent observations, only U has been correlated with pollutant concentrations whereas in those studies where the effect of turbulent fluctuations has been considered, the fluctuations have been found to be more important for pollutants concentrations than the mean flow. Previously Choi et al. (2016) found σ_w to be the strongest determinant factor for ultrafine particle number concentrations in Los Angeles (US) and Weber et al. (2013) in Essen (Germany) whereas Borge et al. (2016) demonstrated strong correlation between NO_2 and u_* (derivative of $\overline{u'w'}$).

3.4. Formation of pollutant hotspots

Previous analysis focused on examining the effect of environmental factors on pollutant concentrations at the different driving routes but it did not tell what are the most important variables for the formation of pollutant hotspots at the street network. Their formation is demonstrated with the aid of our case examples for LDSA and N (Fig. 5). In both examples, higher concentrations focused on north-west part of the main street canyon and around OS in summer. In winter, more hotspots could be observed at the main street canyon when compared to summer. Naturally for different measurement periods, the highest concentrations could be seen in different locations. In order to examine what environmental variables are mostly responsible for variations in each 4-m grid, a multi-linear regression was conducted between the variables, and LDSA, N, BC and NO_x concentrations. Good model performances with RMSE 0.043–0.279 $\mu m^2\ cm^{-3}$, 0.038–0.351 $10^3\,cm^{-3}$, 0.044–0.261 $\mu g\ m^{-3}$ and 0.0420–0.300 ppb, respectively, were found. During summer campaign, $\overline{u'w'}$ was responsible for most of the variation in 70 % (LDSA), 75 % (N), 40 % (BC) and 46 % (NO_x) of the grids. These were followed by traffic rate in 21 % (LDSA), 14 % (N), 35 % (BC) and 42 % (NO_x) of the grids. In winter, on the other hand, more variation in the most determinant variables were seen. For aerosol variables, T_{air} was the most important variable in 64 % (LDSA), 45 % (N) and 35 % (BC) of the grids. For LDSA and N this was followed by Q_H in 12 % and 18 % of the grids emphasising the importance of thermal effects on pollutant dispersion. In the case of BC, $\overline{u'w'}$ was most important variable in 27 % of the grids. For NO_x, $\overline{u'w'}$ was the most important variable in 43 % of the grids, followed by traffic rate in 19 % of the grids. Thus in winter, thermal effects contributed mostly to the local behaviour of aerosol particles whereas in summer mechanical turbulence had more importance for all pollutants. This might be due to the well mixed lower boundary layer throughout the measurements whereas during winter campaign more variability in mixing levels could be seen between the different times of day. The turbulent fluctuations were more important for the formation of hotpots than the mean flow. The importance of thermal turbulence on pollutant distributions within street canyon network has been studied in the past in wind-tunnels and idealised urban areas (Li et al., 2021), but so far experimental evidence from real urban street canyons has been lacking to a large extent.

3.5. Vertical variability of LDSA

The measured vertical LDSA profiles showed large variability in surface (at 4 m) and background concentrations (at >1.5 building height) as well as in their shape (Fig. 6). The surface values varied from 14 to 64 $\mu m^2\ cm^{-3}$ and the background values from 8 to 40 $\mu m^2\ cm^{-3}$. Statistically non-significant differences between the summer and winter surface and background concentrations were observed as based on Mann-Whitney U test. LDSA measured by the drone at four meter height matched well with the reference measurements at the ground level at SS and OS, and on the roof at OS (Supplementary material Fig. 2). When profiles were normalised (Eq. (5)), LDSA followed the exponential decay better in summer than in winter in which case the largest normalised LDSA were not necessarily measured at the surface but rather at elevated level indicating poor vertical mixing of the pollutants. Thus the decay functions worked better in well-mixed situations when compared to more stable situations.

When fitting the first-order exponential decay equation to the normalised profiles, we got k varying between 0.546 and 3.518 corresponding to k_1 values of 0.029–0.186 m^{-1} (Fig. 6 in the Supplementary material). On average k/k_1 were 12 % larger in summer (1.262/0.067 m^{-1}) than in winter (1.124/0.060 m^{-1}). This indicates more efficient dispersion (greater decay) of LDSA from the street canyon in summer than in winter reducing the street-canyon concentrations.

The upper range of k_1 values corresponded those obtained earlier for the same site (0.164 and 0.237 m^{-1}) for two vertical profiles of LDSA when wind was perpendicular to the street canyon (Kuuluvainen et al., 2018).

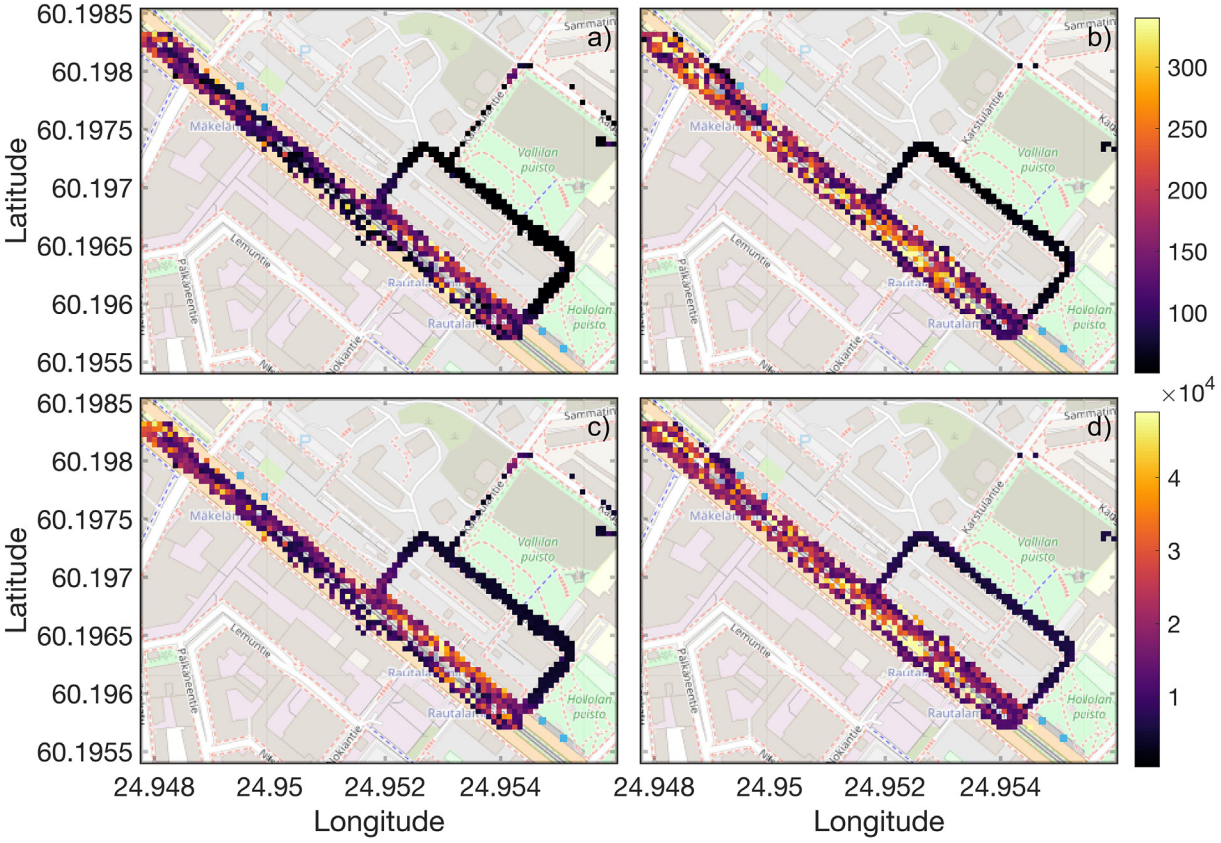

Fig. 5. Example of the spatial variability of a–b) lung deposited surface area (LDSA, $\mu m^2\ cm^{-3}$) and c–d) total particle number concentration (N, cm^{-3}), during case examples in summer (a, c) and winter (b, d).

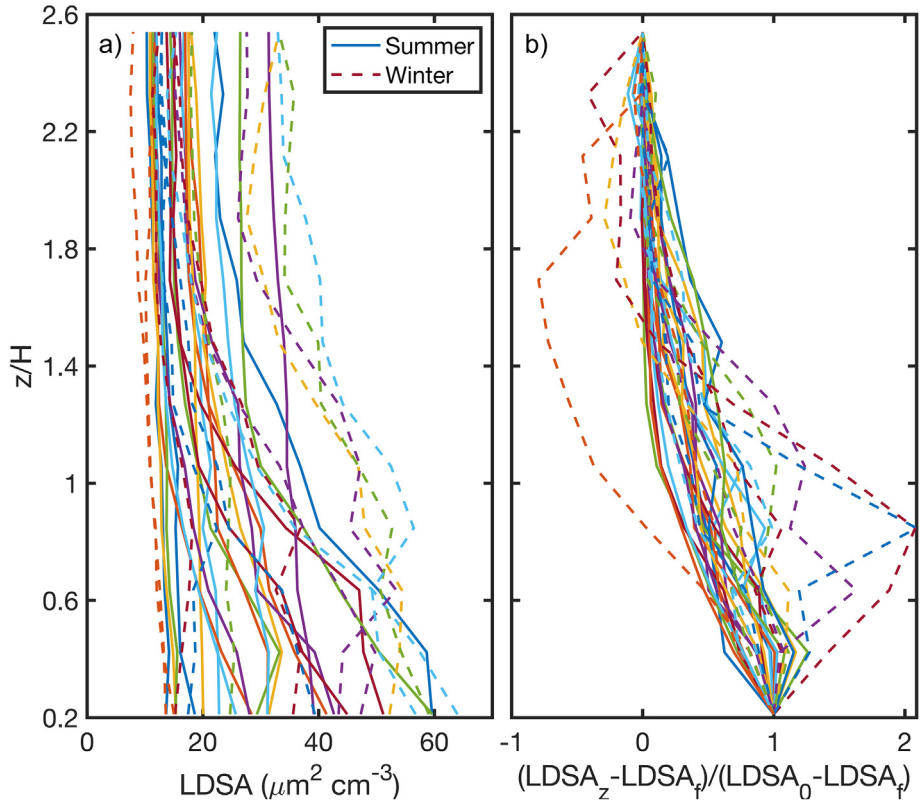

Fig. 6. a) Mean vertical profiles of lung deposited surface area (LDSA) and b) normalised LDSA for summer (solid lines) and winter (dashed lines) measurement campaigns. Geometric mean values for LDSA are used.

In general, our values corresponded well with the range of values obtained in other studies with different morphological and meteorological conditions. In previous studies, the morphological effects to k_1 have been discussed through street canyon aspect ratio (H/W). Murena and Vorraro (2003) found in deep street canyon (H/W = 5.7) k_1 = 0.08–0.16 m^{-1} whereas in more regular street canyons (H/W = 1.65–1) values have been found to range between 0.10 and 0.36 m^{-1} (Chan and Kwok, 2000; Kumar et al., 2008). The street canyon in our case is a wide boulevard type road with H/W = 0.45 for which Kuuluvainen et al. (2018) found larger k_1 and thus stronger mixing than for the canyons with greater H/W-ratio and thus more restricted pollutant ventilation. However, as shown this study with the same H/W-ratio, large variability in k_1 can be found due varying meteorological conditions. Previous studies have classified profiles by wind direction relative to the street canyon of interest (Liu et al., 2021), but we did not find strong dependency of the profile shapes on wind direction.

To demonstrate the variability of the profile shapes, Fig. 7 shows the vertical profiles of LDSA measured using a drone during our case examples. In both cases the LDSA concentrations decreased with height but the behaviour was different between the two sides and case examples. In summer, greater ground level concentrations were measured at OS that at SS. The wind in this case was from North and the forming canyon vortex pushed particles towards northern side of the street-canyon. In winter, on the other hand, the situation was vise versa with greater ground level concentrations at SS side of the street-canyon when the wind was more from west and South-West. Profiles from the two sides united on top of the roof level showing more blended signal. At higher altitudes representing the background (>1.5 times rooftop) the concentrations measured by the drone approached the background values measured at SMEAR III (6.8 and 7.7 $\mu m^2\ cm^{-3}$ in summer and 8.5 and 8.1 $\mu m^2\ cm^{-3}$ in winter during SS and OS measurements, respectively) but remained 34–38 % higher in summer (10.9 and 11.6 $\mu m^2\ cm^{-3}$ at SS and OS) and 45–52 % higher in winter (15.5 and 16.9 $\mu m^2\ cm^{-3}$ at SS and OS). In summer the more efficient mixing could be seen as steeper decay when compared to winter case example.

To get a deeper understanding of the factors affecting the shape of the profiles, i.e., decay of LDSA, a linear regression analysis to the k values was made. The performance of the regression model to predict k did not significantly (with 95 % significance level) improve after five variables identified by the forward feature selection. The five selected variables were T_{air}, U, Q_H, Season and side. The obtained linear regression model

$$k = -3.41 + 2.81T_{air} - 1.89U + 0.88Q_H + 2.00\text{Season} + 0.44\text{side} \quad (6)$$

predicted the variation of k well (RMSE = 0.153 ± 0.010 m^{-1}, see Supplementary material for details). If we have a look on the relative contributions of the different variables in the variation of k, the most contributing variables were T_{air} (2.18) and season (2.00) emphasising the difference in dispersion conditions between summer and winter. These were followed by U with a negative effect (−1.89) and Q_H with a positive effect (0.88). The negative effect of U indicated that with greater mean wind speeds the profile will remain more flat in vertical, and not so pronounced differences between the lower and upper part of the street canyon were seen. Larger Q_H on the other hand indicated more turbulent mixing and unstable

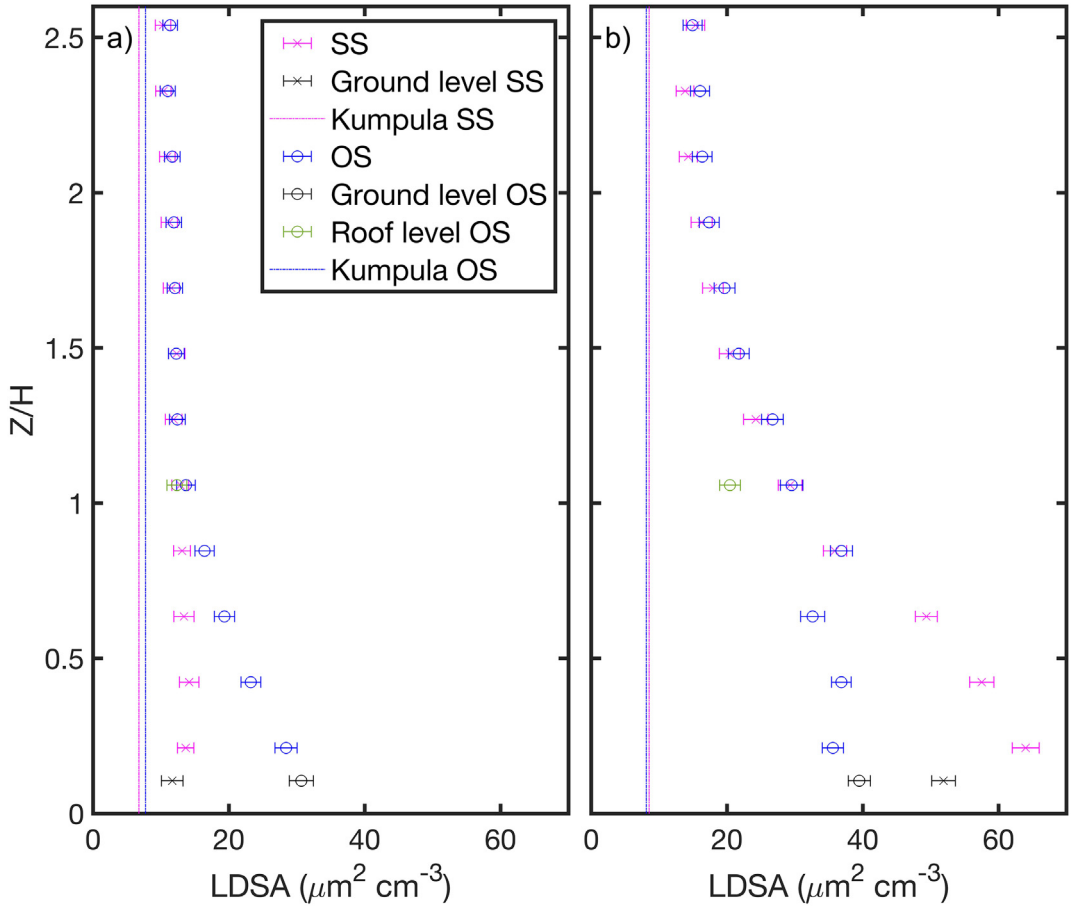

Fig. 7. Vertical distribution of geometric mean lung deposited surface area (LDSA) during our case examples: a) summer profiles measured at the HSY supersite (SS) at 14:57–15:16 and opposite the HSY supersite (OS) at 15:23–15:37 on 14 June 2017, and b) winter profiles measured at SS at 16:01–16:22 and OS at 16:26–16:46 on 5 December 2017. Solid and dashed lines show the background LDSA measured in SMEARIII Kumpula when the drone was measuring at SS and OS, respectively, black markers independent LDSA measurements made at the ground level and green markers independent LDSA measurements made at roof level at OS.

atmosphere resulting in more efficient mixing of pollutants from the surface to the atmosphere. The measurement side was the least important variable (0.44). Interestingly, the surface concentration of LDSA nor traffic rate were among the selected variables indicating minor impact from the emission source itself on the shape of the profile. Neither mechanical turbulent fluctuations appeared among the five variables indicating that for the vertical mean shape of LDSA the mean flow was more significant. One should notice that as all drone measurements were made in low wind speed conditions due to safety reasons, the importance of thermal processes was likely greater that would be with greater wind speeds (Wang et al., 2014). Barbano et al. (2021) studied turbulent vertical exchanges in a deep street canyon ($H/W = 1.65$) in Italy and found thermal processes to be faster than mechanical processes particularly for perpendicular directions. They also found that turbulent exchanges are not important on parallel flow conditions where on contrary the mean flow has been found to dominate (Karttunen et al., 2020).

4. Conclusions

In this study, mobile laboratory and drone measurements of air pollutant concentrations from Helsinki were analysed to examine the horizontal and vertical variability of pollutant distributions, and the effect of environmental conditions on the observed variations. The data were collected during two 2-week measurement campaigns conducted in summer (5–16 Jun) and winter (27 Nov–8 Dec) 2017. Mobile laboratory Sniffer measured the total number concentration (N), lung-deposited surface area (LDSA), black carbon (BC), NO_x and O_3 within a wide street canyon ($H/W = 0.45$) and its immediate surroundings. Drone was used to measure the vertical distribution of LDSA on both sides of the main street canyon.

Meteorological conditions between the two measurement campaigns were contrasting particularly from the point of view of thermal processes. In winter, solar radiation levels were much lower than in summer resulting in lower air temperatures, less turbulence and less mixed lower atmosphere. Mixing started around 3 h later in the morning in winter than in summer, and unstable conditions occurred only 55 % on midday's compared to 92 % occurrence in summer. Mechanical turbulence was also slightly greater in summer than in winter.

The largest concentrations with most temporal variability were measured at the main street canyon for all other pollutants except O_3 which had highest concentrations at the background. For N and BC, higher concentrations were measured in winter than in summer contrary to LDSA which had higher concentrations in summer similarly to O_3. The concentration levels in the street canyon were more affected by traffic when the mobile laboratory was moving with the traffic fleet. At other driving routes, mean concentrations were more affected by the meteorological variables. Both mean wind and turbulence contributed to the variation of pollutant concentrations. For aerosol metrics representative more for the smaller particles, it was more often turbulence which dominated over mean flow. The importance of thermal processes was largest when the mobile van was standing at the HSY supersite or opposite it. The formation of pollutant hotspots within the street canyon network were most controlled by mechanical effects and traffic rate in summer. In winter, the importance of thermal effects increased in the case of LDSA and N. This highlights the need to consider also thermal processes when high-resolution air quality observations in cities are examined.

The measured vertical LDSA profiles showed large variability in their shape, and surface and background concentrations. In summer the profiles followed the predicted exponential decay better than in winter indicating that the decay functions work better in well-mixed conditions compared to more stable conditions. We derived a prediction equation for the decay which is applicable for the H/W ratio of the studied street-canyon. The most important variable controlling the decay function was the season followed by mean flow and thermal turbulence. This study showed the effect of meteorological conditions on vertical profiles to be large indicating that when drawing conclusions for their generalised behaviour, meteorological effects need to be included in addition to morphological effects.

The results show that in order to understand pollutant dispersion in street-canyon networks in detail, not only the mean flow but also turbulent processes should be considered. Mechanical processes were often dominating thermal processes but still both should be accounted for when examining pollutant dispersion in urban areas. This is among the first studies providing experimental evidence on this. In order to understand in detail the effect of meteorological conditions on temporal and spatial variability in both horizontal and vertical directions, more observations from real urban environments from different morphological situations would be needed. Prediction equation for decay functions was derived in this study but more work on the format of the regression model used should be made. We chose a simple linear regression model over other models for its interpretability and as we were interested on the dominant environmental factors over exact prediction equations.

This study focused on the horizontal and vertical dispersion of particle emissions of traffic. The studied metrics N, LDSA and BC in urban environments are dominated by relatively small particles originated from exhaust of vehicles powered by internal combustion engines. However, traffic contributes also the ambient concentrations of extremely small particles not studied here (i.e., nanoclusters, see Hietikko et al., 2018), on the other hand, larger particles such as road dust, brake dust and tyre dust. The processes affecting the dispersion of these particle types may differ from the processes affecting the dispersion of N, LDSA and BC, which should be taken into account in future studies and when exploiting the results of this study.

CRediT authorship contribution statement

Leena Järvi: Conceptualization, Methodology, Formal analysis, Writing – original draft. **Mona Kurppa:** Conceptualization, Investigation, Writing – review & editing. **Heino Kuuluvainen:** Conceptualization, Methodology, Investigation, Writing – review & editing. **Topi Rönkkö:** Resources, Writing – review & editing. **Sasu Karttunen:** Investigation, Writing – review & editing. **Anna Balling:** Software, Writing – review & editing. **Hilkka Timonen:** Investigation, Resources, Writing – review & editing. **Jarkko V. Niemi:** Investigation, Resources, Writing – review & editing. **Liisa Pirjola:** Conceptualization, Methodology, Writing – review & editing.

Data availability

Data will be made available on request.

Declaration of competing interest

The authors declare that they have no known competing financial interests or personal relationships that could have appeared to influence the work reported in this paper.

Acknowledgements

We thank Helsinki Metropolitan Region Urban Research Program, the Academy of Finland CousCOUS project (decision numbers: 332177 and 332178), the Academy of Finland ACCC Flagship (decision numbers: 337549, 337552 and 337551) and the Cityzer project funded by Tekes and Finnish companies (decision number: 2883/31/2015). This project has also received funding from the European Union's Horizon 2020 research and innovation programme under grant agreement No 101036245. The authors are very grateful to Aleksi Malinen and Sami Kulovuori from the Metropolia University of Applied Sciences for operation of the mobile laboratory Sniffer, and Aeromon Oy for conducting the drone measurements. Harri Portin and Anu Kousa from the Helsinki Region Environmental Services Authority (HSY) as well as the HSY's AQ measurement team are acknowledged for their valuable work related to the data quality control and measurements at the HSY supersite. Petri Blomqvist from the City of Helsinki is acknowledged for the traffic count data.

Appendix A. Supplementary data

Supplementary data to this article can be found online at https://doi.org/10.1016/j.scitotenv.2022.158974.

References

Aalto, P., Hämeri, K., Becker, E., Weber, R., Salm, J., Mäkelä, J.M., Hoell, C., O'dowd, C.D., Hansson, H.C., Väkevä, M., Koponen, I.K., Buzorius, G., Kulmala, M., 2001. Physical characterization of aerosol particles during nucleation events. Tellus Ser. B Chem. Phys. Meteorol. 53, 344–358. https://doi.org/10.3402/tellusb.v53i4.17127.

Amato, F., Pérez, N., López, M., Ripoll, A., Alastuey, A., Pandolfi, M., Karanasiou, A., Salmatonidis, A., Padoan, E., Frasca, D., Marcoccia, M., Viana, M., Moreno, T., Reche, C., Martins, V., Brines, M., Minguillón, M., Ealo, M., Rivas, I., van Drooge, B., Benavides, J., Craviotto, J., Querol, X., 2019. Vertical and horizontal fall-off of black carbon and within urban blocks. Sci. Total Environ. 686, 236–245. https://doi.org/10.1016/j.scitotenv.2019.05.434.

Barbano, F., Brattich, E., Di Sabatino, S., 2021. Characteristic scales for turbulent exchange processes in a real urban canopy. Bound.-Layer Meteorol. 178, 119–142. https://doi.org/10.1007/s10546-020-00554-5.

Barlow, J.F., Harman, I.N., Belcher, S.E., 2004. Scalar fluxes from urban street canyons. Part I: Laboratory simulation. Bound.-Layer Meteorol. 113, 369–385. https://doi.org/10.1007/s10546-004-6204-8.

Barreira, L.M.F., Helin, A., Aurela, M., Teinilä, K., Friman, M., Kangas, L., Niemi, J.V., Portin, H., Kousa, A., Pirjola, L., Rönkkö, T., Saarikoski, S., Timonen, H., 2021. In-depth characterization of submicron particulate matter inter-annual variations at a street canyon site in northern Europe. Atmos. Chem. Phys. 21, 6297–6314. https://doi.org/10.5194/acp-21-6297-2021.

Borge, R., Narros, A., Artíñano, B., Yagüe, C., Gómez-Moreno, F.J., de la Paz, D., Román-Cascón, C., Díaz, E., Maqueda, G., Sastre, M., Quaassdorff, C., Dimitroulopoulou, C., Vardoulakis, S., 2016. Assessment of microscale spatio-temporal variation of air pollution at an urban hotspot in Madrid (Spain) through an extensive field campaign. Atmos. Environ. 140, 432–445. https://doi.org/10.1016/j.atmosenv.2016.06.020.

Britter, R.E., Hanna, S.R., 2003. Flow and dispersion in urban areas. Annu. Rev. Fluid Mech. 35, 469–496. https://doi.org/10.1146/annurev.fluid.35.101101.161147.

Chan, L., Kwok, W., 2000. Vertical dispersion of suspended particulates in urban area of Hong Kong. Atmos. Environ. 34, 4403–4412. https://doi.org/10.1016/S1352-2310(00)00181-3.

Choi, W., Ranasinghe, D., Bunavage, K., DeShazo, J., Wu, L., Seguel, R., Winer, A.M., Paulson, S.E., 2016. The effects of the built environment, traffic patterns, and micrometeorology on street level ultrafine particle concentrations at a block scale: results from multiple urban sites. Sci. Total Environ. 553, 474–485. https://doi.org/10.1016/j.scitotenv.2016.02.083.

Eeftens, M., Phuleria, H.C., Meier, R., Aguilera, I., Corradi, E., Davey, M., Ducret-Stich, R., Fierz, M., Gehrig, R., Ineichen, A., Keidel, D., ProbstHensch, N., Ragettli, M.S., Schindler, C., Künzli, N., Tsai, M.Y., 2015. Spatial and temporal variability of ultrafine particles, NO2, PM2.5, PM2.5 absorbance, PM10 and PMcoarse in swiss study areas. Atmos. Environ. 111, 60–70. https://doi.org/10.1016/j.atmosenv.2015.03.031.

Enroth, J., Saarikoski, S., Niemi, J., Kousa, A., Ježek, I., Močnik, G., Carbone, S., Kuuluvainen, H., Rönkkö, T., Hillamo, R., Pirjola, L., 2016. Chemical and physical characterization of traffic particles in four different highway environments in the Helsinki metropolitan area. Atmos. Chem. Phys. 16, 5497–5512. https://doi.org/10.5194/acp-16-5497-2016.

Fenger, J., 2009. Air pollution in the last 50 years - from local to global. Atmos. Environ. 43, 13–22. https://doi.org/10.1016/j.atmosenv.2008.09.061.

Fierz, M., Meier, D., Steigmeier, P., Burtscher, H., 2014. Aerosol measurement by induced currents. Aerosol Sci. Technol. 48, 350–357. https://doi.org/10.1080/02786826.2013.875981.

Fung, P.L., Zaidan, M.A., Timonen, H., Niemi, J.V., Kousa, A., Kuula, J., Luoma, K., Tarkoma, S., Petäjä, T., Kulmala, M., Hussein, T., 2021. Evaluation of white-box versus black-box machine learning models in estimating ambient black carbon concentration. J. Aerosol Sci. 152, 105694. https://doi.org/10.1016/j.jaerosci.2020.105694.

Hietikko, R., Kuuluvainen, H., Harrison, R.M., Portin, H., Timonen, H., Niemi, J.V., Rönkkö, T., 2018. Diurnal variation of nanocluster aerosol concentrations and emission factors in a street canyon. Atmos. Environ. 189, 98–106. https://doi.org/10.1016/j.atmosenv.2018.06.031.

Järvi, L., Junninen, H., Karppinen, A., Hillamo, R., Virkkula, A., Mäkelä, T., Pakkanen, T., Kulmala, M., 2008. Temporal variations in black carbon concentrations with different time scales in Helsinki during 1996–005. Atmos. Chem. Phys. 8 (1017–1027), 2008. https://doi.org/10.5194/acp-8-1017-.

Järvi, L., Hannuniemi, H., Junninen, H., Aalto, Pasi, P., Hillamo, R., Mäkelä, T., Keronen, P., Siivola, E., Vesala, T., Kulmala, M., 2009. The urban measurement station smear iii: continuous monitoring of air pollution and surface-atmosphere interactions in Helsinki, Finland. Boreal Environ. Res. 14, 86–109.

Karttunen, S., Kurppa, M., Auvinen, M., Hellsten, A., Järvi, L., 2020. Large-eddy simulation of the optimal street-tree layout for pedestrian-level aerosol particle concentrations - a case study from a city-boulevard. Atmos. Environ. X 6, 100073. https://doi.org/10.1016/j.aeaoa.2020.100073.

Kittelson, D., Watts, W., Johnson, J., 2004. Nanoparticle emissions on Minnesota highways. Atmos. Environ. 38, 9–19. https://doi.org/10.1016/j.atmosenv.2003.09.037.

Kumar, P., Fennell, P., Britter, R., 2008. Measurements of particles in the 5–1000 nm range close to road level in an urban street canyon. Sci. Total Environ. 390, 437–447. https://doi.org/10.1016/j.scitotenv.2007.10.013.

Kumar, P., Ketzel, M., Vardoulakis, S., Pirjola, L., Britter, R., 2011. Dynamics and dispersion modelling of nanoparticles from road traffic in the urban atmospheric environment – a review. J. Aerosol Sci. 42, 580–603. https://doi.org/10.1016/j.jaerosci.2011.06.001.

Kurppa, M., Hellsten, A., Auvinen, M., Raasch, S., Vesala, T., Järvi, L., 2018. Ventilation and air quality in city blocks using large-Eddy simulation-urban planning perspective. Atmosphere 9. https://doi.org/10.3390/atmos9020065.

Kurppa, M., Roldin, P., Strömberg, J., Balling, A., Karttunen, S., Kuuluvainen, H., Niemi, J.V., Pirjola, L., Rönkkö, T., Timonen, H., Hellsten, A., Järvi, L., 2020. Sensitivity of spatial aerosol particle distributions to the boundary conditions in the PALM model system 6.0. Geosci. Model Dev. 13, 5663–5685. https://doi.org/10.5194/gmd-13-5663-2020.

Kuula, J., Kuuluvainen, H., Niemi, J.V., Saukko, E., Portin, H., Kousa, A., Aurela, M., Rönkkö, T., Timonen, H., 2020. Long-term sensor measurements of lung deposited surface area of particulate matter emitted from local vehicular and residential wood combustion sources. Aerosol Sci. Technol. 54, 190–202. https://doi.org/10.1080/02786826.2019.1668909.

Kuuluvainen, H., Rönkkö, T., Järvinen, A., Saari, S., Karjalainen, P., Lähde, T., Pirjola, L., Niemi, J.V., Hillamo, R., Keskinen, J., 2016. Lung deposited surface area size distributions of particulate matter in different urban areas. Atmos. Environ. 136, 105–113. https://doi.org/10.1016/j.atmosenv.2016.04.019.

Kuuluvainen, H., Poikkimäki, M., Järvinen, A., Kuula, J., Irjala, M., Dal Maso, M., Keskinen, J., Timonen, H., Niemi, J.V., Rönkkö, T., 2018. Vertical profiles of lung deposited surface area concentration of particulate matter measured with a drone in a street canyon. Environ. Pollut. 241, 96–105. https://doi.org/10.1016/j.envpol.2018.04.100.

Lange, M., Suominen, H., Kurppa, M., Järvi, L., Oikarinen, E., Savvides, R., Puolamäki, K., 2021. Machine-learning models to replicate large-eddy simulations of air pollutant concentrations along boulevard-type streets. Geosci. Model Dev. 14 (7411–7424), 2021. https://doi.org/10.5194/gmd-14-7411-.

Lappi, M., Moisio, M., Palonen, M., Marjamäki, M., Ntziachristos, L., Virtanen, A., Ristimäki, J., Keskinen, J., 2002. Electrical filter stage for the ELPI. SAE Int. https://doi.org/10.4271/2002-01-0055.

Li, Z., Ming, T., Liu, S., Peng, C., de Richter, R., Li, W., Zhang, H., Wen, C.Y., 2021. Review on pollutant dispersion in urban areas-part a: effects of mechanical factors and urban morphology. Build. Environ. 190, 107534. https://doi.org/10.1016/j.buildenv.2020.107534.

Liu, X., Shi, X.Q., He, H.D., Li, X.B., Peng, Z.R., 2021. Vertical distribution characteristics of particulate matter beside an elevated expressway by unmanned aerial vehicle measurements. Build. Environ. 206, 108330. https://doi.org/10.1016/j.buildenv.2021.108330.

Murena, F., Vorraro, F., 2003. Vertical gradients of benzene concentration in a deep street canyon in the urban area of Naples. Atmos. Environ. 37, 4853–4859. https://doi.org/10.1016/j.atmosenv.2003.08.033.

Nordbo, A., Järvi, L., Vesala, T., 2012. Revised eddy covariance flux calculation methodologies - effect on urban energy balance. Tellus Ser. B Chem. Phys. Meteorol. 64, 18184. https://doi.org/10.3402/tellusb.v64i0.18184.

Oberdorster, G., Oberdorster, E., Oberdorster, J., 2005. Nanotoxicology: an emerging discipline evolving from studies of ultrafine particles. Environ. Health Perspect. 113, 823–839. https://doi.org/10.1289/ehp.7339.

Pirjola, L., Parviainen, H., Hussein, T., Valli, A., Hämeri, K., Aalto, P., Virtanen, A., Keskinen, J., Pakkanen, T., Mäkelä, T., Hillamo, R., 2004. "Sniffer" - a novel tool for chasing vehicles and measuring traffic pollutants. Atmos. Environ. 38, 3625–3635. https://doi.org/10.1016/j.atmosenv.2004.03.047.

Pirjola, L., Lähde, T., Niemi, J., Kousa, A., Rönkkö, T., Karjalainen, P., Keskinen, J., Frey, A., Hillamo, R., 2012. Spatial and temporal characterization of traffic emissions in urban microenvironments with a mobile laboratory. Atmos. Environ. 63, 156–167. https://doi.org/10.1016/j.atmosenv.2012.09.022.

Ranstam, J., Cook, J.A., 2018. Lasso regression. BJ. (British Journal of Surgery) 105. https://doi.org/10.1002/bjs.10895 1348–1348.

Rivas, I., Kumar, P., Hagen-Zanker, A., de Fatima Andrade, M., Slovic, A.D., Pritchard, J.P., Geurs, K.T., 2017. Determinants of black carbon, particle mass and number concentrations in London transport microenvironments. Atmos. Environ. 161, 247–262. https://doi.org/10.1016/j.atmosenv.2017.05.004.

Rivas, I., Beddows, D.C., Amato, F., Green, D.C., Järvi, L., Hueglin, C., Reche, C., Timonen, H., Fuller, G.W., Niemi, J.V., Perez, N., Aurela, M., Hopke, P.K., Alastuey, A., Kulmala, M., Harrison, R.M., Querol, X., Kelly, F.J., 2020. Source apportionment of particle number size distribution in urban background and traffic stations in four european cities. Environ. Int. 135, 105345. https://doi.org/10.1016/j.envint.2019.105345.

Ruths, M., von Bismarck-Osten, C., Weber, S., 2014. Measuring and modelling the local-scale spatio-temporal variation of urban particle number size distributions and black carbon. Atmos. Environ. 96, 37–49. https://doi.org/10.1016/j.atmosenv.2014.07.020.

Solomon, P.A., Vallano, D., Lunden, M., LaFranchi, B., Blanchard, C.L., Shaw, S.L., 2020. Mobile-platform measurement of air pollutant concentrations in California: performance assessment, statistical methods for evaluating spatial variations, and spatial representativeness. Atmos. Meas. Tech. 13, 3277–3301. https://doi.org/10.5194/amt-13-3277-2020.

Vardoulakis, S., Fisher, B.E., Pericleous, K., Gonzalez-Flesca, N., 2003. Modelling air quality in street canyons: a review. Atmos. Environ. 37, 155–182. https://doi.org/10.1016/S1352-2310(02)00857-9.

Vardoulakis, S., Gonzalez-Flesca, N., Fisher, B.E., Pericleous, K., 2005. Spatial variability of air pollution in the vicinity of a permanent monitoring station in central Paris. Atmos. Environ. 39, 2725–2736. https://doi.org/10.1016/j.atmosenv.2004.05.067 fourth International Conference on Urban Air Quality: Measurement, Modelling and Management, 25-28 March 2003.

Wang, Y., Zhong, K., Zhang, N., Kang, Y., 2014. Numerical analysis of solar radiation effects on flow patterns in street canyons. Eng. Appl. Comput. Fluid Mech. 8, 252–262. https://doi.org/10.1080/19942060.2014.11015511.

Weber, S., Kordowski, K., Kuttler, W., 2013. Variability of particle number concentration and particle size dynamics in an urban street canyon under different meteorological conditions. Sci. Total Environ. 449, 102–114. https://doi.org/10.1016/j.scitotenv.2013.01.044.

Yli-Ojanperä, J., Kannosto, J., Marjamäki, M., Keskinen, J., 2010. Improving the nanoparticle resolution of the ELPI. Aerosol Air Qual. Res. 10, 360–366. https://doi.org/10.4209/aaqr.2009.10.0060.